Chinese Chemical Letters 34 (2023) 107595

Contents lists available at ScienceDirect

Chinese Chemical Letters

journal homepage: www.elsevier.com/locate/cclet

Chemical proteomics combined with metabonomics reveals berberine targets NDUFV1 of complex I in the respiratory chain to regulate energy metabolism

Xiaoyao Ma, Yiman Han, Kaixin Liu, Yongping Bai, He Gao, Yuanyuan Hou*, Gang Bai*

State Key Laboratory of Medicinal Chemical Biology, College of Pharmacy and Tianjin Key Laboratory of Molecular Drug Research, Nankai University, Tianjin 300381, China

ARTICLE INFO

Article history:
Received 26 January 2022
Revised 6 June 2022
Accepted 6 June 2022
Available online 13 June 2022

Keywords:
Berberine
Photoaffinity labeled
Chemical proteomics
NDUFV1
Complex I
Energy metabolism

ABSTRACT

Berberine (BBR) is the primary alkaloid compound of the heat-clearing traditional Chinese medicine Huanglian (*Coptis chinensis*) and exerts regulatory effects on energy metabolism. However, the specific targets and molecular mechanisms are not clear. In this paper, the BBR-affected energy metabolism pathway was screened by nontargeted metabolomics, and a BBR-derived photoaffinity labeled (PAL) probe was designed to identify potential targets *via* a chemical proteomics approach. NDUFV1, a subunit of complex I on mitochondria, was identified as a potential target of BBR. In the respiratory chain, BBR suppressed the activity of complex I, reduced the electrochemical potential in the mitochondrial intermembrane and inhibited the generation of ATP and heat *via* competitive binding with NDUFV1. The results illustrated the underlying mechanism of BBR in the downregulation of energy metabolism.

Coptis chinensis (*C. chinensis*, Huanglian in Chinese) is a famous traditional herbal medicine that has been used for clearing heat and detoxification in traditional Chinese medicine for thousands of years [1]. The crude extract of *C. chinensis* reduces oxygen consumption and energy metabolism in mice [2]. Berberine (BBR) is the primary alkaloid compound of *C. chinensis* and has a wide range of pharmacological properties, such as anti-inflammatory and antidiabetic properties, and alleviates digestive and cardiovascular diseases [3]. Recent research has also shown that the oral administration of BBR decreases ATP levels to regulate the energy metabolism network [4]. However, few studies have revealed the specific targets and molecular mechanisms by which BBR regulates energy metabolism.

Chemical proteomics, and in particular photoaffinity labeled (PAL), is a valuable tool for identifying protein-ligand interactions [5,6]. PAL is always used in chemical probes that can covalently bind to the target in response to activation by light, which enables us to study the hydrophobic targets of noncovalent kinetic small molecules [7,8]. In this study, we performed nontargeted metabolomics combined with a chemical proteomics approach, which was achieved with a BBR-derived PAL probe, to analyze the potential target proteins in regulating mitochondrial energy metabolism. Subsequent molecular biology research revealed the mechanism by which BBR inhibits oxidative respiratory chain function.

The animal experiments were approved by the Animal Ethics Committee, Nankai university (Tianjin, China) and were performed in accordance with the guidelines of the national legislation of China. The use and care of mice for the study described herein was approved (2021-SYDWLL-000227). The material information and detailed experimental procedures are described in Supporting information.

First, we investigated the metabolites and related pathways that BBR affected in HepG2 cells by nontargeted metabolomics. The significantly different metabolites compared to the control (Con) group identified by screening are shown in a volcano figure (Fig. 1A), and the functions and the degree of enrichment according to the KEGG metabolic pathway were analyzed. The significance of their enrichment in each pathway was calculated using Fisher's exact test. As shown in Fig. 1B, the oxidative phosphorylation pathway and the central carbon metabolism pathway, which are related to energy metabolism, were markedly affected by BBR. There were 7 significantly different metabolites in energy metabolism-related pathways. After treatment with BBR, the content of ADP increased markedly (Fig. 1C), and the content of ATP and the ratio of ATP/ADP decreased markedly in the oxidative phosphorylation pathway (Figs. 1D and E). In the central carbon metabolism

* Corresponding authors.
E-mail addresses: houyy@nankai.edu.cn (Y. Hou), gangbai@nankai.edu.cn (G. Bai).

https://doi.org/10.1016/j.cclet.2022.06.018
1001-8417/

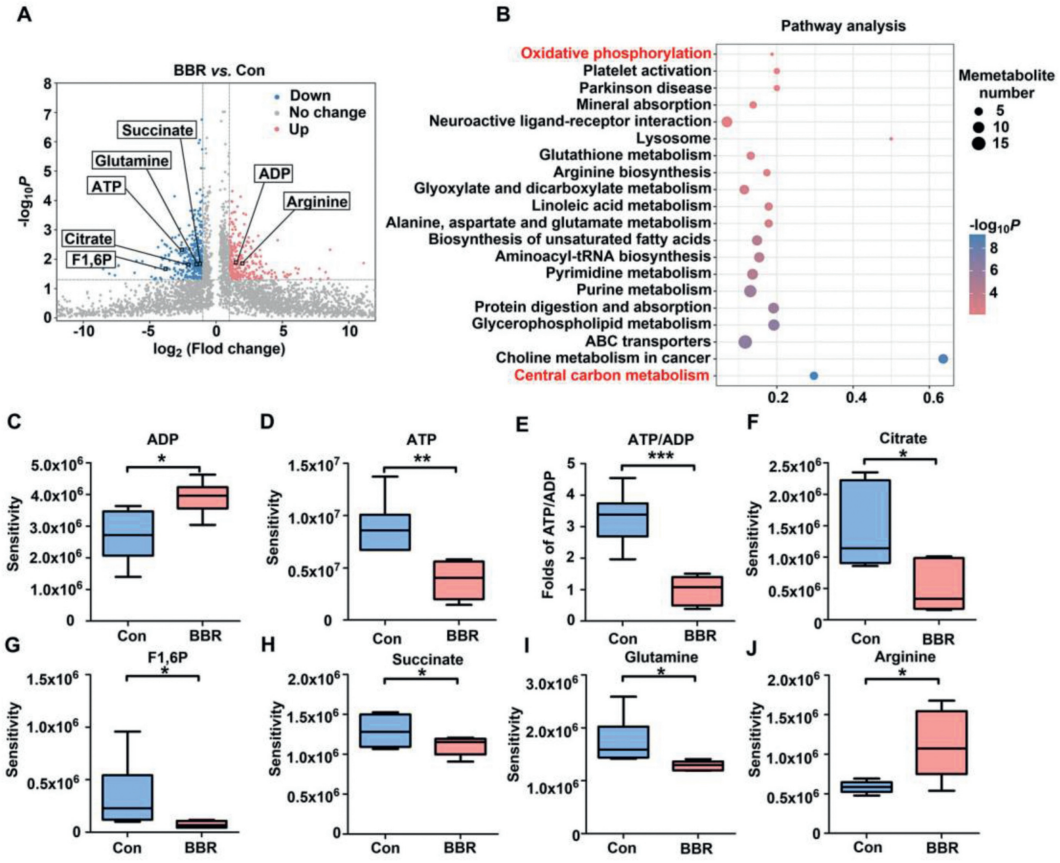

Fig. 1. Nontargeted metabolomics analysis of the metabolites in HepG2 cells. (A) Screening of significantly different metabolites affected by BBR in cells. (B) Metabolic pathway enrichment of the significantly different metabolites. Metabolite sensitivity analysis of (C) ADP and (D) ATP and (E) the ratio of ATP/ADP in the oxidative phosphorylation pathway. Metabolite sensitivity analysis of (F) citrate, (G) F1,6P, (H) succinate, (I) glutamine and (J) arginine in the central carbon metabolism pathway is presented as the mean ± SD ($n = 6$, * $P < 0.05$, ** $P < 0.01$, *** $P < 0.001$ compared to the Con group).

pathway, the contents of citrate, fructose 1,6-bisphosphate (F1,6P), succinate and glutamine were significantly reduced, and the content of arginine was significantly enhanced with BBR treatment (Figs. 1F-J). Citrate and succinate participate in the tricarboxylic acid (TCA) cycle, which together with oxidative phosphorylation form the primary ATP synthesis harboring pathways in mitochondria [9]. The results suggested that oxidative phosphorylation and TCA were potential pathways affected by BBR in the process of regulating energy metabolism.

To analyze the main target of BBR in mitochondria, we synthesized a BBR-PLA probe, which contained the skeleton structure of BBR, an alkynyl click tag and a photoaffinity group (Fig. 2A). The synthesis route of the BBR-PLA probe is shown in Scheme S1 and the location analysis of BBR-PLA probe in HepG2 cells is shown in Fig. S1 (Supporting information). As shown in Fig. 2B, the probe (1 μmol/L) or DMSO was incubated in mitochondria, which were extracted from the livers of mice using a kit, with or without BBR (10 μmol/L) for 4 h. The mitochondria were irradiated at 365 nm to induce optical crosslinking. Finally, azide-modified magnetic microspheres (MMs) were used to enrich proteins following lysis by click reaction, and the targets were identified by LC-MS analysis. The enrichment proteins were analyzed by SDS-PAGE. Compared to DMSO (Lane 2, negative Con group) and BBR-PAL probes with the addition of BBR (Lane 4, competition group), BBR-PAL probes (Lane 3) enriched more proteins, which were suggested to be potential targets of BBR (Fig. 2C). Then, LC-MS was used to identify the captured proteins and analyze the potential targets of BBR. In the proteomics analysis, the scores of the captured proteins in the BBR-PAL probe group were compared to those in the Con and competition groups. According to the screening results, there were four significantly different proteins: NADH dehydrogenase ubiquinone flavoprotein 1 (NDUFV1), acetyl-coenzyme A synthetase (ACSS2), oxoglutarate dehydrogenase (DHTK1), and very long-chain specific acyl-CoA dehydrogenase (ACADV) (Fig. 2D). NDUFV1 is a subunit of respiratory complex I, which is the beginning of electron transport in the respiratory chain. The oxidative phosphorylation is accomplished by a series of electron transfer reactions to generate cellular ATP in the respiratory chain [10]. Moreover, ACSS2, DHTK1 and ACADV are not related with oxidative phosphorylation and TCA pathways. This result suggested that NDUFV1 was a potential target of BBR in the respiratory chain.

To further verify the result of target screening, Western blots were used to confirm the most likely target of NDUFV1 enrichment. As expected, the approximately 51-kDa NDUFV1 protein band was enriched in the BBR-PAL probe group compared to the Con and competition groups. The repeated targeting fishing ($n = 3$) suggested NDUFV1 was a potential target protein of BBR (Fig. 3A). In the co-localization detection, the pseudo-green fluorescence of the BBR-PAL probe was observed only in the BBR-PAL probe and competition group, and weakened with the addition of BBR. In addition, the distribution of NDUFV1, which was stained pseudo-red with a Cy3 antibody, was observed in cells. After amplification, fluorescent imaging showed that the BBR-PAL probe appeared to co-localize with the NDUFV1 protein partially (*pseudo*-yellow) (Fig. 3B). The above results were consistent with the target screening result and suggested that BBR and the BBR-PAL probe competitively bound with NDUFV1 in mitochondria. As a core subunit, the function of NDUFV1 is related to the activity of complex I [11].

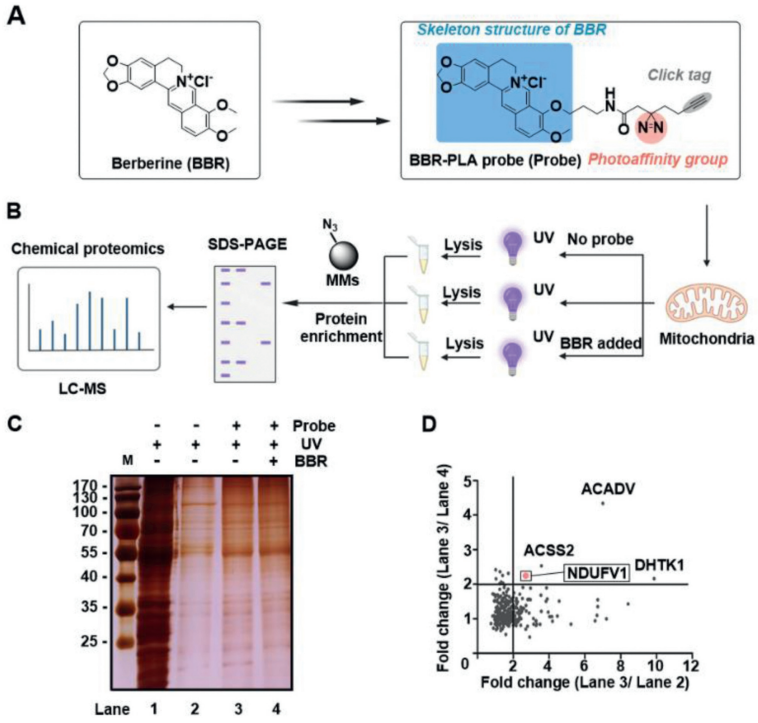

Fig. 2. Target analysis of BBR in the regulation of energy metabolism. (A) The structures of BBR and the BBR-PLA probe. (B) The processes of target fishing and detection from mitochondria by chemical proteomics. (C) SDS-PAGE of silver staining was used to detect the proteins enriched from mitochondria (Lane 1, total mitochondrial lysate; Lane 2, Con group; Lane 3, BBR-PAL probe group; Lane 4, competition group). (D) Scatter diagram of differential protein profiling captured in the BBR-PAL probe group compared to the Con and competition groups.

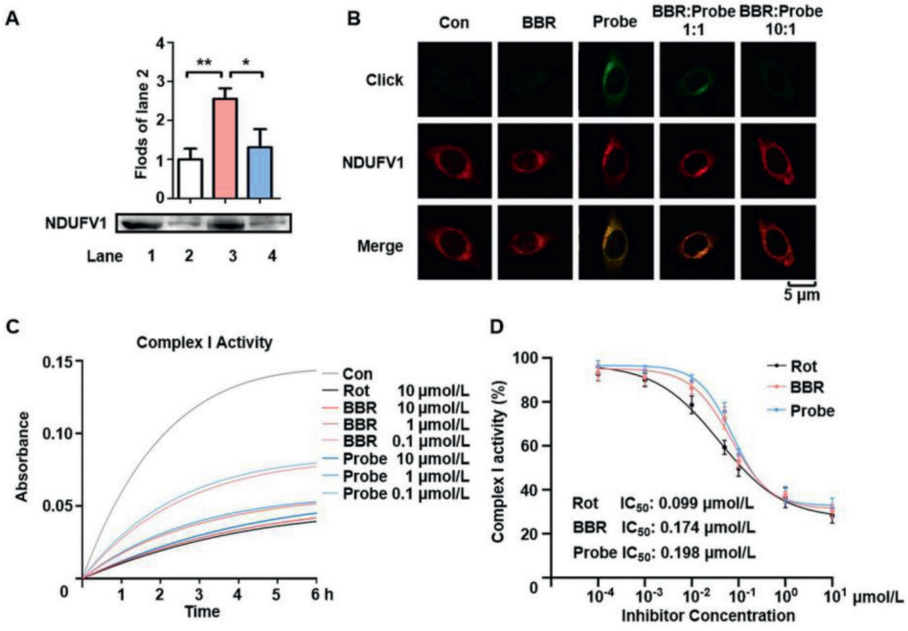

Fig. 3. NDUFV1 was identified as the energy metabolism target of BBR. (A) Western blot analysis was used to detect NDUFV1 among the enriched proteins from mitochondria (Lane 1, the total mitochondrial lysate; Lane 2, Con group; Lane 3, BBR-PAL probe group; Lane 4, competition group, $n = 3$, * $P < 0.05$, ** $P < 0.01$ compared to BBR-PAL probe group). (B) The co-localization of NDUFV1 (*pseudo*-red) and the BBR-PAL probe (*pseudo*-green) in HepG2 cells. Effects (C) and IC_{50} (D) of Rot, BBR and the BBR-PAL probe on the complex I activity.

Thus, the activity of complex I in HepG2 cells was measured using a kit. As shown in Fig. 3C, BBR and the BBR-PAL probe both inhibited the complex I activity in a dose-dependent manner. The IC_{50} of BBR and BBR-PAL were 0.174 μmol/L and 0.198 μmol/L (Fig. 3D), which suggested BBR-PAL maintained similar inhibitory effects as BBR on the inhibition of complex I activity. Combined with the target analysis, these results indicated that the BBR and BBR-PAL probes both affected the complex I activity by binding with NDUFV1.

Complex I is the entry point of electrons into the respiratory chain and, together with complex III and complex IV, couples electron transfer and pumps protons from the mitochondrial matrix to

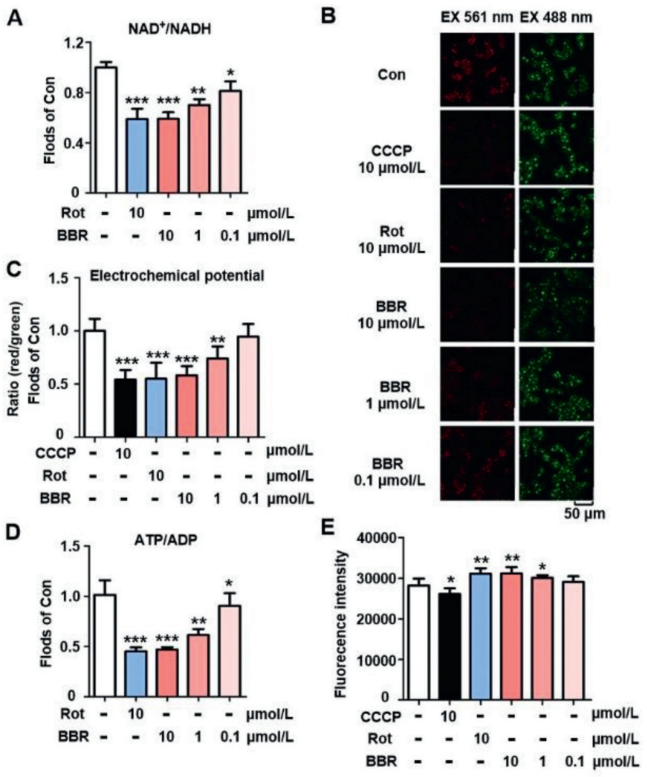

Fig. 4. BBR regulated energy metabolism by inhibiting complex I. (A) The content ratio of NAD^+/NADH in HepG2 cells. Fluorescence imaging (B) and statistics (C) of electrochemical potential in the mitochondrial intermembrane. (D) The content ratio of ATP/ADP in HepG2 cells. (E) Mitochondrial temperature analysis with the RhBIV fluorescent probe ($n = 6$, * $P < 0.05$, ** $P < 0.01$, *** $P < 0.001$ compared to the Con group).

the intermembrane space, which builds up an electrochemical potential [12]. The electrochemical potential is dissipated as heat and ATP by uncoupling protein (UCP) and complex V (ATP synthase) [13]. According to the biological process, we analyzed the effect of BBR on energy metabolism in the respiratory chain. As shown in Fig. 4A, the complex I inhibitors rotenone (Rot) and BBR both reduced the generation of NAD^+ from NADH by inhibiting complex I in HepG2 cells. The accumulated proton potential in the mitochondrial intermembrane was evaluated by JC-1 probe, and the uncoupler carbonyl cyanide-m-chlorophenylhydrazone (CCCP) promoted protons back to the mitochondrial matrix and induced a decrease in the ratio of pseudo-red fluorescence to pseudo-green fluorescence, which indicated electrochemical potential. Rot and BBR also decreased the fluorescence ratio and the electrochemical potential in the mitochondrial intermembrane (Figs. 4B and C). Then, the translation of ADP to ATP was inhibited by Rot and BBR in a dose-dependent manner (Fig. 4D). The RhBIV probe, a small-molecule fluorescent mitochondrial thermometer, was then used to detect the mitochondrial temperature in cells [14]. CCCP uncoupled oxidative phosphorylation in mitochondria and generated heat, which caused the intensity of fluorescence to be reduced. Rot and BBR enhanced the intensity of fluorescence, which suggested that the release of thermal energy decreased (Fig. 4E). The above results indicated that BBR affected energy metabolism in the respiratory chain by inhibiting complex I.

Complex I contributes to cellular energy generation by transferring electrons from NADH to ubiquinone coupled to proton translocation across the mitochondrial inner membrane [15]. NADH interacts with flavin mononucleotide (FMN) in NDUFV1, and FMN accepts two electrons simultaneously from NADH and transfers them to ubiquinone *via* Fe-S clusters [16]. To clarify the molecular mechanism by which BBR inhibits complex I, microscale thermophoresis (MST) was performed to analyze the relationship of BBR and FMN in NDUFV1. As shown in Fig. 5A, BBR markedly increased the interaction between FMN and NDUFV1 recombinant protein, and the K_D value was reduced to 31 μmol/L from 611 μmol/L with the addition of 1.25 mmol/L BBR, which suggested that BBR and FMN competitively combined in the same pocket of NDUFV1 (Fig. 5A). Molecular docking was used to provide additional insights into the interaction of BBR and NDUFV1 (PDB: 5LDX). In all cases, the top-scoring poses of BBR and FMN were displayed as 3D maps, and the estimated free binding energy of BBR (−8.92 kcal/mol) was lower than that of FMN (−6.58 kcal/mol) (Fig. 5B). In the thermal shift assay, BBR and FMN both increased the thermal stability of the NDUFV1 recombinant protein. BBR caused a 1.8 °C increase in the protein melting temperature (ΔT), which was slightly higher than

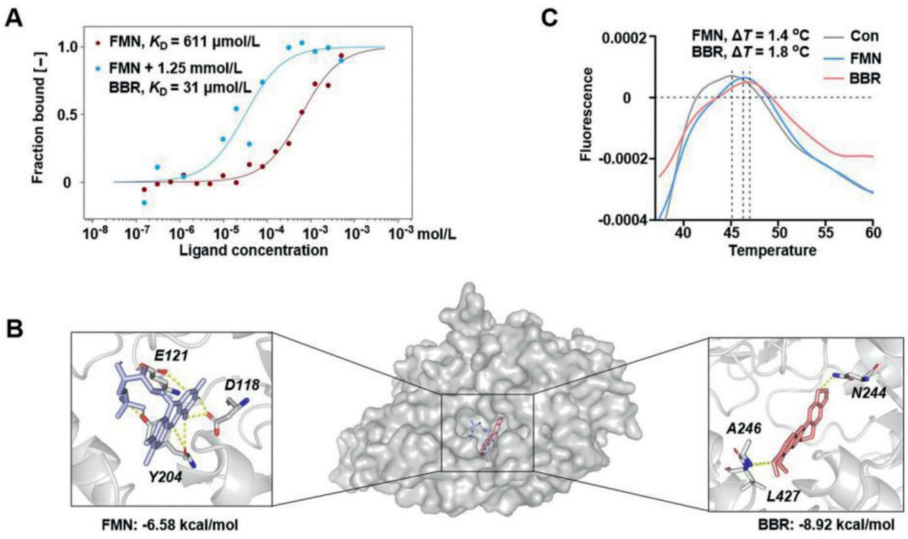

Fig. 5. Analysis of the potential mechanism by which BBR inhibits the activity of complex I. (A) The interactions of FMN and NDUFV1 recombinant protein with or without the addition of 1.25 mmol/L BBR were determined by MST. (B) Molecular modeling of NDUFV1 with BBR or FMN. PyMOL software was used to display the 3D maps of the interaction of NDUFV1 with BBR or FMN. BBR (red) and FMN (blue) are displayed as sticks. (C) The thermal stability of the NDUFV1 recombinant protein incubated with BBR or FMN was assessed using the thermal shift assay.

that caused by FMN (1.4 °C) (Fig. 5C). The above results revealed that the affinity between BBR and NDUFV1 was stronger than that of FMN, which indicated that BBR might prevent FMN from binding with NDUFV1 and interacting with NADH to inhibit the production of electrons and the activity of complex I.

The respiratory chain contains five complexes, I-V, which are all made up of multiple subunits [17]. For example, complex I, which contains 55 subunits, is one of the largest membrane protein complexes and includes 14 central subunits, an L-shaped structure with 7 subunits in the hydrophilic peripheral arm and another 7 in the membrane arm, and 31 accessory subunits in the structure of complex I [10,11]. Hence, it is challenging to identify the specific subunit proteins of BBR targets in the respiratory chain. In our study, we designed a novel alkyne- and diazirine-containing BBR-PAL probe. When a transient protein-small molecule structure exists, active diazirine can attack the protein *via* 365 nm UV irradiation to generate a protein-probe complex for further enrichment and proteomics analysis [18]. This probe helps us efficiently identify the target subunit of BBR that regulates energy metabolism in the respiratory chain.

The activity of complex I directly affects the generation of ATP and heat; it is also related to glucose and lipid metabolism [19,20]. Recent studies have illustrated the potential mechanism by which BBR attenuated fatty acid consumption, β-oxidation and lipogenesis and improved glucose homoeostasis *via* inhibition of complex I in diabetic animals [21,22]. However, few studies have revealed the subunit of the BBR target in complex I. To the best of our knowledge, we show for the first time that BBR suppresses the activity of complex I by competitively binding with the NDUFV1 subunit. These results provide information to develop BBR derivatives for the treatment of disorders related to energy metabolism based on the oxidative respiratory chain by targeting NDUFV1 of complex I.

The electron transfer from NADH to ubiquinone in complex I requires the presence of at least eight Fe-S clusters, and the interruption of the transfer process by the inhibitor induces the leakage of one electron to molecular oxygen and generates reactive oxygen species (ROS) [23,24]. Rot targets the NUOD subunit and inhibits the activity of complex I by blocking electron transfer. This leads to an increase in ROS content, subsequent mitochondrial DNA damage and cell death [25]. However, BBR prevents the interaction of the electron donors FMN and NADH in NDUFV1 and inhibits the generation of electrons at the beginning of the transfer process, which suppresses the production of ROS. This is consistent with the low toxicity of BBR in the clinic [26]. The evidence in the present study also indicated that BBR was a potential complex I inhibitor *in vivo*.

In this study, a BBR-PAL probe showed a powerful capacity for target capture, and the NDUFV1 subunit of complex I was identified as a putative target. Our results demonstrated that BBR inhibited complex I activity and reduced the generation of ATP and heat *via* competitive binding with NDUFV1. In summary, these results provide an increased understanding of BBR, particularly regarding the molecular mechanism of the regulation of energy metabolism.

Declaration of competing interest

The authors declare that they have no known competing financial interests or personal relationships that could have appeared to influence the work reported in this paper.

Acknowledgments

This research was supported by the National Natural Science Foundation of China (No. 81973449) and the China Postdoctoral Science Foundation (No. 2020M680871).

Supplementary materials

Supplementary material associated with this article can be found, in the online version, at doi:10.1016/j.cclet.2022.06.018.

References

[1] Y.H. Yang, C.T. Vong, S. Zeng, et al., Ethnopharmacol 268 (2021) 113573.
[2] C.P. Zhou, J.B. Wang, X.R. Zhang, et al., Sci. China C: Life Sci. 52 (2009) 1073–1080.
[3] D.Y. Song, J.Y. Hao, D.M. Fan, Front. Med. 14 (2020) 564–582.
[4] Y. Yu, W.W. Cai, J. Zhou, et al., Int. Immunopharmacol. 87 (2020) 106830.
[5] Y. Ren, Q.S. Sun, Z.G. Yuan, et al., Chin. Chem. Lett. 30 (2019) 1233–1236.
[6] J.T. Du, J. Guo, D.W. Kang, et al., Chin. Chem. Lett. 31 (2020) 1695–1708.
[7] J. Wang, Q.H. Chen, Y.Y. Shan, et al., Drug Discov. Today 25 (2020) 133–140.
[8] G.D. Hu, H.Y. Jia, L.N. Zhao, et al., Chin. Chem. Lett. 30 (2019) 1704–1716.
[9] A.M. Bliek, M.M. Sedensky, P.G. Morgan, Genetics 207 (2017) 843–871.
[10] K. Fiedorczuk, J.A. Letts, G. Degliesposti, et al., Nature 538 (2016) 406–410.
[11] K. Parey, C. Wirth, J. Vonck, et al., Curr. Opin. Struct. Biol. 63 (2020) 1–9.
[12] R.Y. Guo, S. Zong, M. Wu, et al., Cell 170 (2017) 1247–1257.
[13] M.J. Berardi, W.M. Shih, S.C. Harrison, et al., Nature 476 (2011) 109–113.
[14] F.K. Shen, W. Yang, J. Cui, et al., Anal. Chem. 93 (2021) 13417–13420.
[15] J.M. Berrisford, R. Baradaran, L.A. Sazanov, Biochim. Biophys. Acta (BBA) - Bioenerg. 1857 (2016) 892–901.
[16] Y.E. Galemou, H. Angerer, K. Parey, et al., Biochim. Biophys. Acta (BBA) - Bioenerg. 1861 (2020) 148153.
[17] R.Y. Guo, J.K. Gu, S. Zong, et al., Biomed. J. 41 (2018) 9–20.
[18] H.M. Zhang, Y.L. Song, Y. Zou, et al., Chem. Commun. 50 (2014) 4891–4894.
[19] M. Alimujiang, X.Y. Yu, M.Y. Yu, et al., J. Cell. Mol. Med. 24 (2020) 5758–5771.
[20] A.J. Worth, S.S. Basu, N.W. Snyder, et al., J. Biol. Chem. 289 (2014) 26895–26903.
[21] M.Y. Yu, M. Alimujiang, L.L. Hu, et al., Int. J. Biol. Sci. 17 (2021) 1693–1707.
[22] W.L. Hou, J. Yin, M. Alimujiang, et al., J. Cell. Mol. Med. 22 (2018) 1316–1328.
[23] R. Fato, C. Bergamini, M. Bortolus, et al., Biochim. Biophys. Acta 1787 (2009) 384–392.
[24] L. Kussmaul, J. Hirst. Proc. Natl. Acad. Sci. U. S. A. 103 (2006) 7607–7612.
[25] E. Darrouzet, J.P. Issartel, J. Lunardi, et al., FEBS Lett. 431 (1998) 34–38.
[26] Y.F. Jin, D.B. Khadka, W.J. Cho, Expert. Opin. Ther. Pat. 26 (2016) 229–243.